PHYSICAL REVIEW A **80**, 012711 (2009)

Charge transfer in collisions of C^{2+} carbon ions with CO and OH targets

E. Bene,[1] P. Martínez,[2] G. J. Halsáz,[3] Á. Vibók,[4] and M. C. Bacchus-Montabonel[5]
[1]*Institute of Nuclear Research, Hungarian Academy of Sciences, P.O. Box 51, H-4001 Debrecen, Hungary*
[2]*Departamento de Química, Laboratorio Asociado al CIEMAT de Física Atómica y Molecular en Plasmas de Fusión, Universidad Autónoma de Madrid, Madrid 28049, Spain*
[3]*Department of Information Technology, University of Debrecen, P.O. Box 12, H-4010 Debrecen, Hungary*
[4]*Department of Theoretical Physics, University of Debrecen, P.O. Box 5, H-4010 Debrecen, Hungary*
[5]*Laboratoire de Spectrométrie Ionique et Moléculaire, CNRS et Université de Lyon, 43 Boulevard du 11 Novembre 1918, 69622 Villeurbanne Cedex, France*
(Received 6 May 2009; published 24 July 2009)

The charge transfer in collisions of C^{2+} ions with the CO molecule and the OH radical has been studied theoretically by means of *ab initio* quantum chemistry molecular methods followed by a semiclassical dynamical treatment in the keV collision energy range. The comparison of the cross sections calculated for these two collision systems exhibits interesting features with regard to the anisotropy of these processes and the influence of the vibration of the molecular target.

DOI: 10.1103/PhysRevA.80.012711 PACS number(s): 34.70.+e

I. INTRODUCTION

In the action of ionizing radiation with biological tissue, damage has been shown to be induced by the secondary particles, low-energy electrons, radicals, or singly- and multiply-charged ions, generated along the track after interaction of the ionizing radiation with the biological medium [1]. Theoretical and experimental studies have been developed in order to understand the different mechanisms involved, in particular a number of recent works has been devoted to collisions between ions and biomolecular systems [2–7]. In these reactions, generally at relatively low energies, different processes have to be considered: excitation and fragmentation of the molecule, ionization of the gaseous target, and also possible charge transfer from the multicharged ion toward the biomolecule. The excitation and fragmentation cross sections are determined experimentally from mass spectra. But charge transfer has been shown to be a complementary process and can be investigated theoretically in the framework of the molecular representation of the collisions. Such studies provide important information on the mechanism as well as on the electronic structure of the projectile and target during the reaction, as shown in recent work on collisions of C^{q+} ions on uracil and halouracil molecules [5–7].

Mainly direct processes, where the ions are colliding with a biomolecule, have been, up to now, investigated [2–7]. But, from a biophysical point of view [8], very important damage may be due to indirect processes where ions are interacting with the medium, generally the water solvent, or the environment and can generate very reactive species. The action of ions on water molecules produces, for example, OH radicals which can, in turn, induce severe damage by interaction with the biological environment. In that sense, we have investigated two test case reactions: the $C^{2+}+OH \rightarrow C^{+}+OH^{+}$ collision modeling the action of ions on OH radicals created in the medium and the $C^{2+}+CO \rightarrow C^{+}+CO^{+}$ charge transfer in order to have a look to some possible indirect processes. In a previous study of the $C^{2+}+OH$ collision in a linear approach [9], the influence of the geometry of the molecular target has been investigated, in particular a characteristic mechanism has been pointed out for very constrained geometries of the OH radical. However, a number of effects have to be taken into account in such processes, in particular the consideration of the orientation of the target toward the projectile. Effectively, in previous studies on direct collisions of C^{q+} ions on uracil and halouracil molecules, charge transfer has been shown to be highly anisotropic with electron delocalization from the target to the colliding ion [5–7]. We have thus undertaken an analysis of the two charge-transfer processes $C^{2+}+OH$ and $C^{2+}+CO$ with consideration of the orientation of the projectile toward the target, as well as possible variations of the geometry of the target molecule. The influence of rotational coupling has also been investigated and a detailed comparison between both collision systems has been performed in order to extract some more general features of these processes. *Ab initio* molecular calculations of the potentials and couplings followed by a semiclassical dynamics are performed.

II. THEORETICAL TREATMENT

A. Molecular calculations

For both systems, the geometry may be described by the internal Jacobi coordinates $\{R,r,\alpha\}$ with the origin at the center of mass of the target molecule, as defined in Fig. 1. The diatomic molecule corresponds, respectively, to $AB=OH$ for the $C^{2+}+OH$ system and $AB=OC$ for the $C^{2+}+CO$ one such as, in the linear approach, the collision of the C^{2+} ion toward the oxygen atom would correspond to an angle $\alpha=180°$ in both cases.

The molecular calculations have been carried out using the MOLPRO suite of *ab initio* programs [10]. The molecular orbitals were optimized in state-averaged complete active space self-consistent field (CASSCF) calculations using the correlation-consistent quadruple zeta aug-cc-AVQZ basis set of Dunning [11]. The active space includes all valence elec-

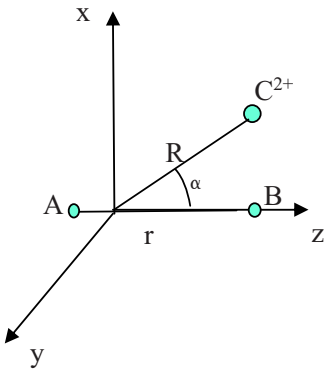

FIG. 1. (Color online) Internal coordinates for the C^{2+}-molecule systems (AB=OH or AB=OC, respectively).

trons distributed among $n=2,3$ orbitals for carbon and oxygen and the 1s orbital for hydrogen; the 1s orbitals of carbon and oxygen are frozen in the calculation. The geometries of the $^2\Pi$ ground state of OH, $^3\Sigma^-$ ground state of OH^+, $^1\Sigma^+$ ground state of CO, and $^2\Sigma^+$ ground state of CO^+ have been optimized at the CASSCF+multireference configuration interaction (MRCI) level of theory. The value used in the calculation for the equilibrium geometry of OH is 1.834 967 a.u. [9], the corresponding value for the equilibrium geometry of CO is 2.140 535 31 a.u., and its vertical ionization potential is 13.76 eV, in good agreement with experimental [12] and previous theoretical values [13,14]. As shown previously for C^{2+}+OH [9], such calculations lead to a good agreement with calculations of separated species taking account of experimental data for carbon ions [15] and calculations at equilibrium geometry for the target molecule and its ion. The corresponding values for the C^{2+}+CO system are presented in Table I. Spin-orbit coupling being negligible in the energy range of interest, we can assume the electron spin to be conserved in the collision process.

The radial coupling matrix elements between all pairs of states of the same symmetry have been calculated by means of the finite difference technique

$$g_{KL}(R) = \langle \psi_K | \partial/\partial R | \psi_L \rangle = \langle \psi_K(R) | \lim_{\Delta \to 0} \frac{1}{\Delta} | \psi_L(R+\Delta) - \psi_L(R) \rangle,$$

which, taking account of the orthogonality of the eigenfunctions $|\psi_K(R)\rangle$ and $|\psi_L(R)\rangle$ for $K \neq L$, reduces to

$$g_{KL}(R) = \langle \psi_K | \partial/\partial R | \psi_L \rangle = \lim_{\Delta \to 0} \frac{1}{\Delta} \langle \psi_K(R) | \psi_L(R+\Delta) \rangle,$$

with the parameter $\Delta=0.0012$ a.u. as previously tested and using the three-point numerical differentiation method for reasons of numerical accuracy. The rotational coupling matrix elements $\langle \psi_K(R)|iL_y|\psi_L(R)\rangle$ between states of angular moment $\Delta\Lambda=\pm 1$ have been calculated directly from the quadrupole moment tensor from the expression $iL_y = x\frac{\partial}{\partial z} - z\frac{\partial}{\partial x}$. The center of mass of the system has been chosen as origin of electronic coordinates.

TABLE I. Comparison of asymptotic energies from separated species calculation at the optimized $CO(^1\Sigma^+)$ distance (in eV).

Configuration	This calculation	Separated species
$C^{2+}(^1S)+CO(^1\Sigma^+)$	11.67	11.81
$C^+(^2P)+CO^+(B\ ^2\Sigma^+)$	6.09	6.09
$C^+(^2P)+CO^+(A^2\Pi)$	3.36	3.37
$C^+(^2P)+CO^+(A\ ^2\Sigma^+)$	0	0

B. Collision dynamics

The collision dynamics has been performed in the keV laboratory energy range where semiclassical approaches using the EIKONXS code [16] may be used with a good accuracy as straight-line trajectories are satisfying for energies above 10 eV/amu [17,18]. At the first level of approximation, electronic transitions are assumed to occur so fast that vibrational and rotational motions can be neglected during the collision. The ion-molecule collision may be visualized as an ion bumping into an anisotropic atom. The total and partial cross sections, corresponding to purely electronic transitions, may then be determined by solving the impact-parameter equation as in the usual ion-atom approach, considering the internuclear distance of the molecular target fixed in a given geometry. Such an approach is, of course, relatively crude, but it has shown its efficiency in a number of ion-diatomics [19,20] and even ion-polyatomics collisions [5,7] in the keV energy range we are dealing with [20]. Such a treatment has been performed for different geometries of the molecular targets OH and CO as well as for different orientations of these targets toward the C^{2+} projectile ion, taking account of all the transitions driven by radial coupling matrix elements. The transitions driven by rotational coupling matrix elements have been analyzed with respect to the collision energies involved in the process. The choice of origin coordinates is expected to be accurate enough for impact velocities lower than 0.5 a.u. (E_{lab}=75 keV) to neglect the translation factors [21,22] in the total cross-section calculations. Such translation effect may be evaluated in the approximation of the common translation factor developed by Errea *et al.* [23]. The radial and rotational coupling matrix elements between states $|\psi_K\rangle$ and $|\psi_L\rangle$ are then transformed, respectively, into

$$\langle \psi_K | \partial/\partial R - (\varepsilon_K - \varepsilon_L) z^2/2R | \psi_L \rangle,$$

$$\langle \psi_K | iL_y + (\varepsilon_K - \varepsilon_L) zx | \psi_L \rangle,$$

where ε_K and ε_L are the electronic energies of states $|\psi_K\rangle$ and $|\psi_L\rangle$ and z^2 and zx the components of the quadrupole moment tensor. As shown previously [24], the translation effect is negligible for collision energies lower than 100 keV and has been evaluated to be less than 3% for the present systems, even at the highest collision velocity v_{coll}=0.6 a.u. (E_{lab}=108 keV).

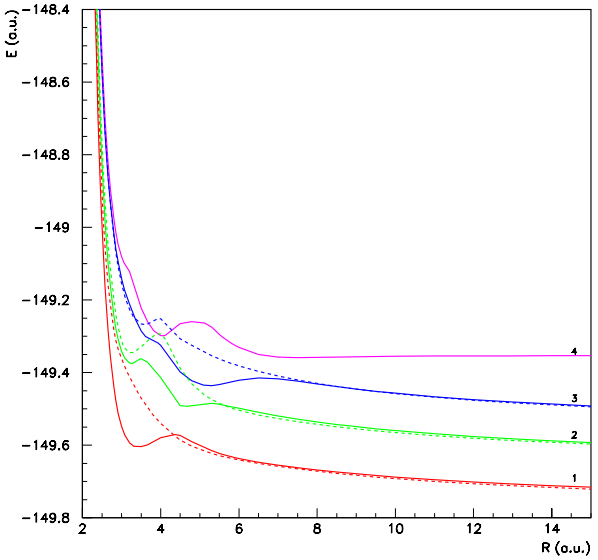

FIG. 2. (Color online) Potential energy curves for the $^1\Sigma^+$ (full line) and $^1\Pi$ (broken line) states of the C^{2+}-CO molecular system at equilibrium, $\alpha=180°$. (1) $C^+(1s^22s^22p)^2P+CO^+(A\ ^2\Sigma^+)$; (2) $C^+(1s^22s^22p)^2P+CO^+(A^2\Pi)$; (3) $C^+(1s^22s^22p)^2P+CO^+(B\ ^2\Sigma^+)$; (4) $C^{2+}(1s^22s^2)^1S+CO(^1\Sigma^+)$ entry channel.

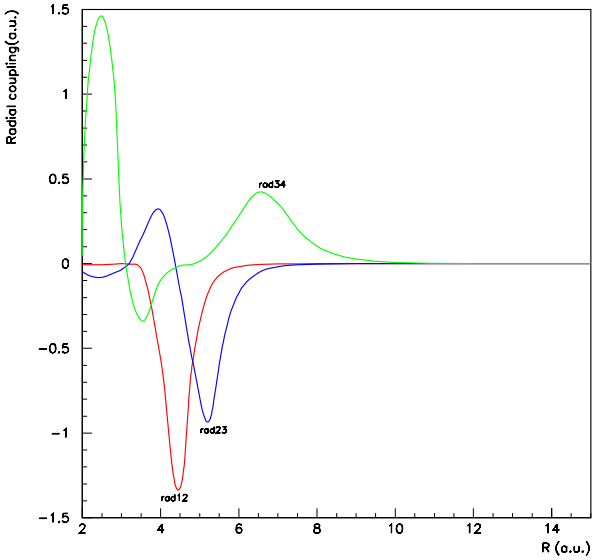

FIG. 3. (Color online) Radial coupling matrix elements for the $^1\Sigma^+$ states of the C^{2+}-CO molecular system at equilibrium, $\alpha=180°$. Same labels as in Fig. 2.

III. RESULTS

A. Rotational effect

The first point in such a study is to assess in which collision energy range our dynamical calculations may be accurate for each system. Effectively, we have to consider all the exit channels corresponding simultaneously to the excited states of the C^+ ion and also all the possible excited states of CO^+ or OH^+, respectively, which could be correlated with the entry channel by means of radial or rotational couplings.

Considering the $C^{2+}(1s^22s^2)^1S+CO(^1\Sigma^+)$ system, the entry channel being of $^1\Sigma^+$ symmetry, only $^1\Sigma^+$ levels could be involved in the process by means of radial coupling and $^1\Pi$ levels by means of rotational coupling. Seven levels are thus to be taken into account with regard to the different excited states of CO^+ [25,26]

$$C^{2+}(1s^22s^2)^1S + CO(^1\Sigma^+) \quad ^1\Sigma^+,$$

$$C^+(1s^22s^22p)^2P + CO^+(B\ ^2\Sigma^+) \quad ^1\Sigma^+, ^1\Pi,$$

$$C^+(1s^22s^22p)^2P + CO^+(A^2\Pi) \quad ^1\Sigma^+, ^1\Pi,$$

$$C^+(1s^22s^22p)^2P + CO^+(A\ ^2\Sigma^+) \quad ^1\Sigma^+, ^1\Pi.$$

The $C^+(1s^22s^22p)^2P+CO^+(B^2\Pi)$ and $C^+(1s^22s2p^2)^2D+CO^+(A\ ^2\Sigma^+)$ channels corresponding to very long-range crossings may be considered as totally diabatic and have not been considered in the calculation. We have first investigated the linear approach with the C^{2+} ion colliding CO toward the oxygen atom, corresponding to the angle $\alpha=180°$. The potential-energy curves for the equilibrium distance, the associated radial couplings between $^1\Sigma^+$ and $^1\Pi$ states, respectively, as well as the rotational couplings have been calculated in the [2.0–15.0] internuclear distance range. The potentials are presented in Fig. 2 and show clearly a relatively smooth avoided crossing between the entry channel and the $^1\Sigma^+\{C^+(1s^22s^22p)^2P+CO^+(B\ ^2\Sigma^+)\}$ exit channel around 7.0 a.u., with a sharper one at short range. Two avoided crossings, around, respectively, 4.5 and 5.0 a.u., may also be observed between the $^1\Sigma^+\{C^+(1s^22s^22p)^2P+CO^+(A\ ^2\Sigma^+)\}$ and $^1\Sigma^+\{C^+(1s^22s^22p)^2P+CO^+(A^2\Pi)\}$ exit channels, as well as between the $^1\Sigma^+\{C^+(1s^22s^22p)^2P+CO^+(A^2\Pi)\}$ and $^1\Sigma^+\{C^+(1s^22s^22p)^2P+CO^+(B\ ^2\Sigma^+)\}$ levels. In correspondence with these avoided crossings, the radial coupling elements between $^1\Sigma^+$ states are exhibiting sharp peaks, as presented in Fig. 3.

In order to check the influence of the rotational coupling interaction in this charge-transfer process, the collision dynamics has been performed in a wide range of velocities, from 0.05 to 0.6 a.u. ([0.75–108] keV laboratory energies). In a first calculation, only the $^1\Sigma^+$ states coupled radially have been taken into account. In a second one, all couplings have been considered, the radial coupling matrix elements between, respectively, $^1\Sigma^+$ and $^1\Pi$ levels, as well as the corresponding rotational couplings. The total cross sections are displayed in Fig. 4. They show clearly that for velocities lower than 0.3 a.u. ($E_{lab}=27$ keV), the rotational effect is negligible and the rotational couplings could be neglected in the collision treatment without introducing a significant error. For higher velocities, the contribution of rotational couplings increases with increasing velocity reaching about 30% of the total cross section at $v_{coll}=0.6$ a.u.. The rotational couplings must then be taken into account in the calculation.

In the case of the $C^{2+}(1s^22s^2)^1S+OH(^2\Pi)$ system, the molecular calculations are very complex. Effectively, the exit channels C^++OH^+ are extremely close in energy and a great number of electronic states have to be taken into account. In this collision system, $^2\Pi$ levels are involved and are correlated with the $^2\Pi\{C^{2+}(1s^22s^2)^1S+OH(^2\Pi)\}$ entry channel by radial coupling. In a first step, the molecular calculation has

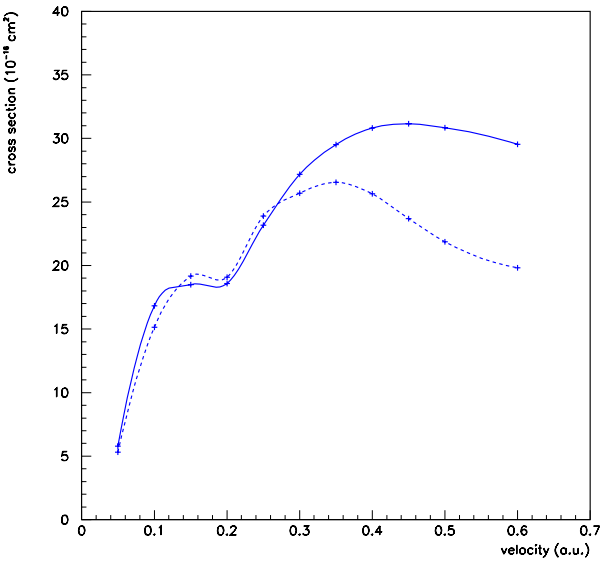

FIG. 4. (Color online) Total charge-transfer cross sections with radial and rotational couplings (full line) and radial couplings between $^1\Sigma^+$ states only (broken line) for the C^{2+}-CO system at equilibrium, $\alpha=180°$.

thus been performed for the $^2\Pi$ states only and molecular states correlated by rotational coupling have not been considered [9]. However, considering the increase of the rotational effect with collision energy, the dynamical treatment has been performed in the reduced [0.05–0.35] a.u. collision velocity range ([0.75–36.75] keV laboratory energies). This work is completed now by introducing the $^2\Sigma^+$ states correlated with the entry channel by means of rotational coupling. The potential-energy curves, radial and rotational couplings in the geometry corresponding to the C^{2+} ion colliding OH toward the oxygen atom ($\alpha=180°$) at equilibrium OH distance, have been calculated in the [2–9.5] a.u. internuclear distances range. The $^2\Pi$ and $^2\Sigma^+$ potentials are presented in Figs. 5(a) and 5(b) and show clearly a very intricate molecular system. The collision dynamics taking into account the radial and rotational interactions may be compared to the previous calculation considering only the radial coupling between $^2\Pi$ levels. The results are presented in Fig. 6 and drive the same conclusions as already pointed out for the C^{2+} +CO collision system: for collision velocities lower than 0.3 a.u., the rotational coupling effect is weak and may be neglected without introducing significant errors in the cross-section values. This justifies *a posteriori* our previous results for the linear approach [9]. As the molecular calculations are extremely complex in the case of the C^{2+}+OH system, we have considered in further work only the $^2\Pi$ states correlated by radial coupling. The rotational effect has been neglected and the dynamic treatment has been reduced to the [0.05–0.3] collision velocity range.

B. Anisotropic effect

The orientation of the projectile toward the molecular target has been studied in detail for the C^{2+}+CO system for geometries corresponding to specific values of the angle α =[180°,135°,90°,45°,0°]. We thus take into account the collision of the C^{2+} projectile in a linear approach toward the oxygen atom of CO ($\alpha=180°$), through a perpendicular collision ($\alpha=90°$), and the reverse linear approach of the projectile toward the carbon atom of CO ($\alpha=0°$). Important features of the potential-energy curves are presented in Figs. 7(a) and 7(b). For $^1\Sigma^+$ states, they show mainly a decrease of the interaction between the entry channel and the $^1\Sigma^+\{C^+(1s^22s^22p)^2P+CO^+(B\ ^2\Sigma^+)\}$ exit channel from the linear $\alpha=180°$ geometry to the perpendicular one, associated

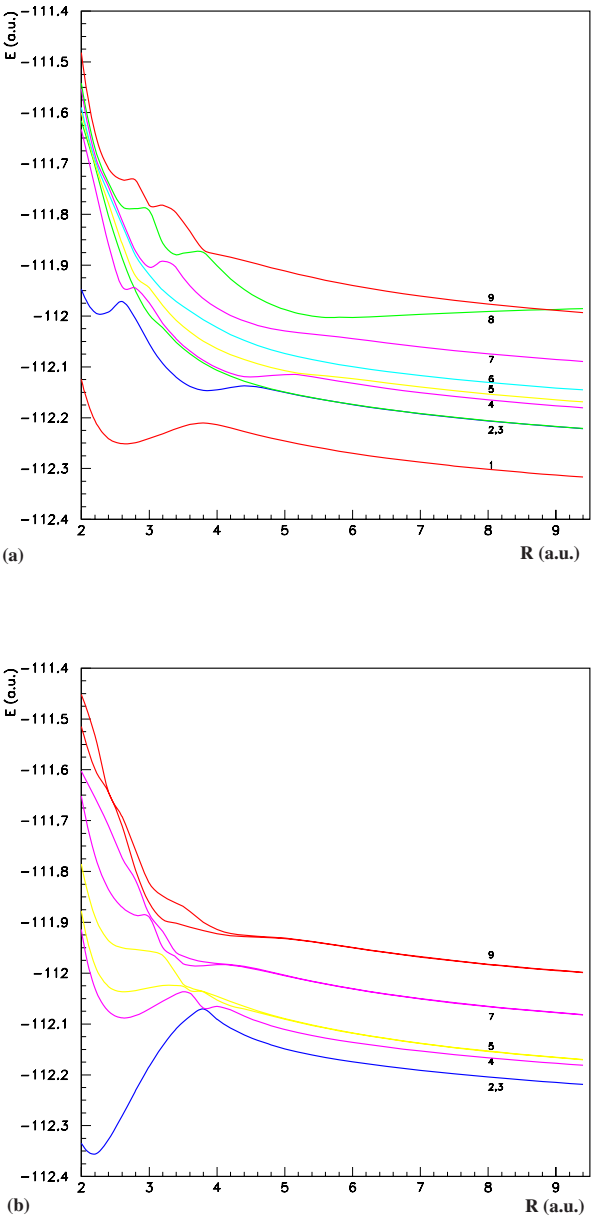

FIG. 5. (Color online) (a) Potential energy curves for the $^2\Pi$ states of the C^{2+}-OH molecular system at equilibrium, $\alpha=180°$. (1) $C^+(^2P)+OH^+(^3\Sigma^-)$ (2,3) $C^+(^2P)+OH^+(^1\Delta)$; (4) $C^+(^2P)+OH^+(^1\Sigma^+)$; (5) $C^+(^2P)+OH^+(^3\Pi)$; (6) $C^+(^4P)+OH^+(^3\Sigma^-)$; (7) $C^+(^2P)+OH^+(^1\Pi)$; (8) $C^{2+}(^1S)+OH(^2\Pi)$ entry channel; (9) $C^+(^4P)+OH^+(^3\Pi)$. (b) Potential energy curves for the $^2\Sigma^+$ states of the C^{2+}-OH molecular system at equilibrium, $\alpha=180°$. Same labels as in (a).

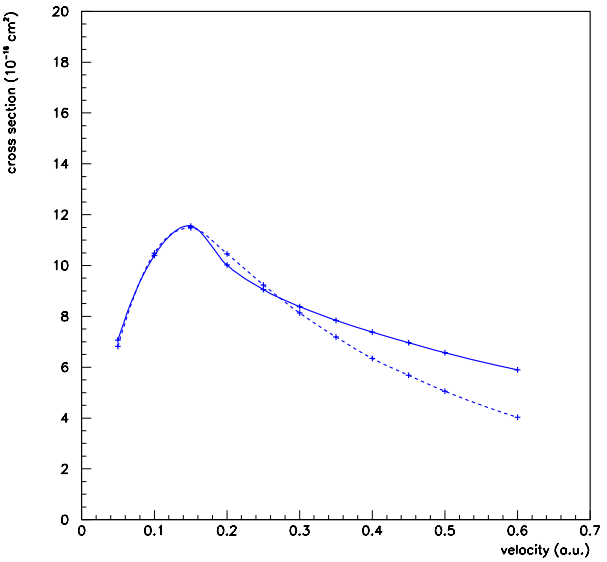

FIG. 6. (Color online) Total charge-transfer cross sections with radial and rotational couplings (full line) and radial couplings between $^2\Pi$ states only (broken line) for the C^{2+}-OH system at equilibrium, $\alpha=180°$.

to a displacement of the avoided crossing to lower internuclear distances. This may be visualized particularly clearly on the radial coupling matrix elements displayed in Fig. 8 where we can observe a strong lowering of the radial coupling for $\alpha=90°$. The orientations $\alpha=45°$ and $\alpha=0°$ for the approach toward the carbon atom of CO appear in correspondence, respectively, to $\alpha=135°$ and $\alpha=180°$ but with lower couplings. An interesting feature may be pointed out for the $^1\Pi$ levels where a strong interaction between the $^1\Pi\{C^+(1s^22s^22p)^2P+CO^+(A^2\Pi)\}$ and $^1\Pi\{C^+(1s^22s^22p)^2P+CO^+(B\ ^2\Sigma^+)\}$ exit channels appear for the $\alpha=135°$ orientation as shown also on the potentials in Fig. 7(a). Such strong coupling is also present for the correspondent $\alpha=45°$ geometry contrary to the linear and perpendicular orientations where corresponding radial couplings between $^1\Pi$ states remain low [Fig. 9].

The collision dynamics for velocities between 0.05 and 0.6 a.u. carried out for the different orientations are presented in Fig. 10. If we consider the cross sections corresponding to an identical approach of the projectile, but, respectively, on the oxygen side or carbon side of the CO molecule, it appears clearly that the collision toward the oxygen atom is more favorable than on the carbon side. This is the case in the linear approach, as well as in the 135° and 45° corresponding orientations. On the contrary, the collision perpendicularly to the molecular target is markedly less efficient. These results are in complete agreement with the variations of the radial couplings between $^1\Sigma^+$ states pointed out in Fig. 8. Furthermore, the reaction in the linear approach toward the oxygen atom is the most efficient collision orientation, particularly at higher energies.

The same conclusions may be driven for the C^{2+}+OH collision system. The potential-energy curves for the linear approach toward the hydrogen atom ($\alpha=0°$) at equilibrium distance OH are presented in Fig. 11. They show globally the same behavior than the potentials obtained for the linear approach toward the oxygen atom ($\alpha=180°$) [9] with however a displacement of the crossing between the entry channel and the $^2\Pi\{C^+(^4P)+OH^+(^3\Pi)\}$ exit channels toward shorter internuclear distances. The cross sections calculated in both orientations are presented in Fig. 12. As already observed for C^{2+}+CO, the preferred approach is the linear collision toward the oxygen atom corresponding to the angle $\alpha=180°$. The values of the cross sections averaged over the different orientations are displayed in Table II for the C^{2+}+CO and C^{2+}+OH collision systems. The collision appears clearly more efficient for C^{2+}+CO with cross sections reaching up to 17. 10^{-16} cm^2. In both cases, the cross sections present a

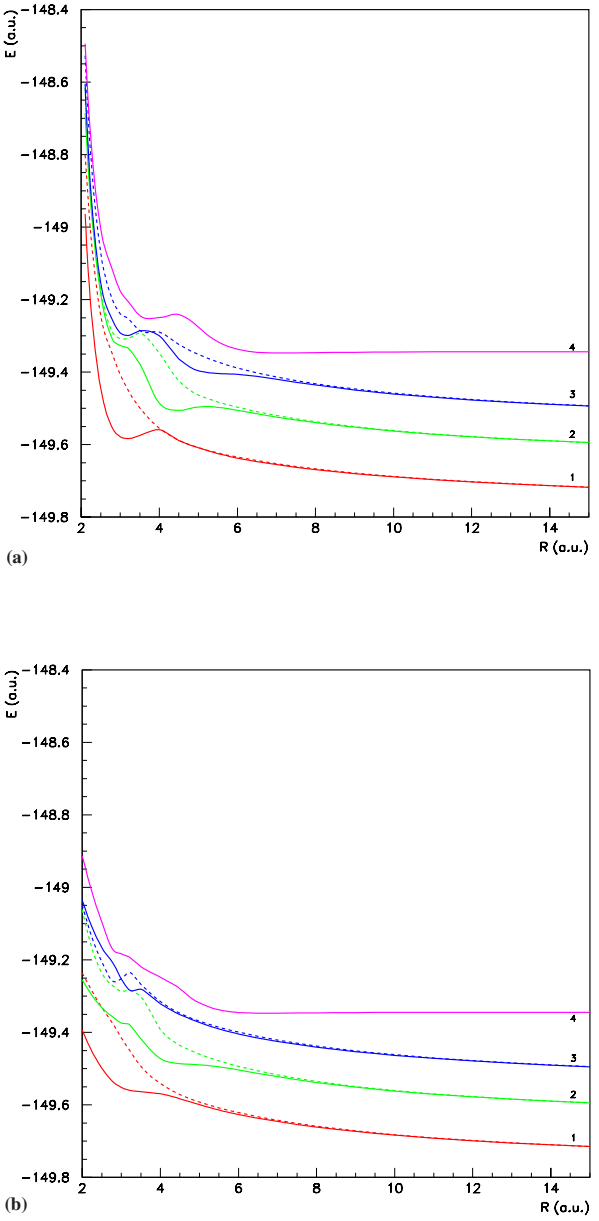

FIG. 7. (Color online) (a) Potential energy curves for the $^1\Sigma^+$ (full line) and $^1\Pi$ (broken line) states of the C^{2+}-CO molecular system at equilibrium, $\alpha=135°$. Same labels as in Fig. 2. (b) Potential energy curves for the $^1\Sigma^+$ (full line) and $^1\Pi$ (broken line) states of the C^{2+}-CO molecular system at equilibrium, $\alpha=90°$. Same labels as in Fig. 2.

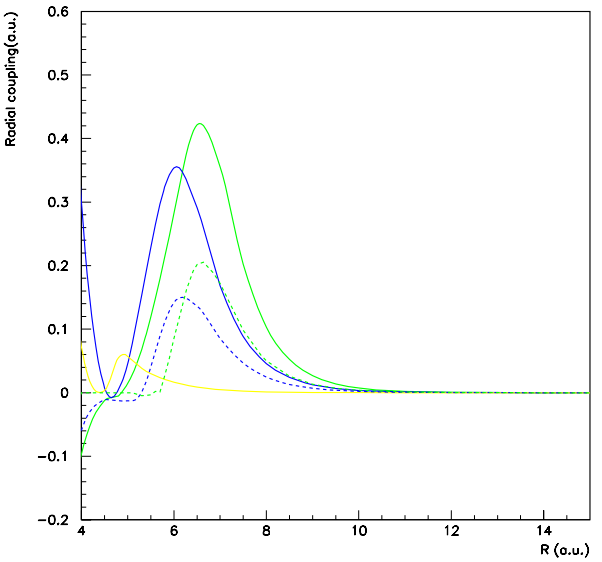

FIG. 8. (Color online) Variation of the g_{34} radial coupling matrix element between $^1\Sigma^+$ levels for different orientations of the C^{2+} projectile toward the CO molecule at equilibrium. Same labels as in Fig. 2. —— α=180° (green); —— α=135° (blue); —— α=90° (yellow); - - - - α=45° (blue); - - - - α=0° (green).

maximum, around v_{coll}=0.2 a.u. for C^{2+}+OH, and at higher energies around v_{coll}=0.5 a.u. for C^{2+}+CO.

C. Vibrational effect

As previously pointed out for the C^{2+}+OH linear reaction [9], the collision of the C^{2+} projectile ion toward the molecular target may also depend of the geometry of the system corresponding to different values of the vibration coordinate r_{CO} or r_{OH}, respectively. The effect appears markedly less significant in the case of the C^{2+}+CO system than already observed on C^{2+}+OH. Effectively, as shown on Fig. 13, the

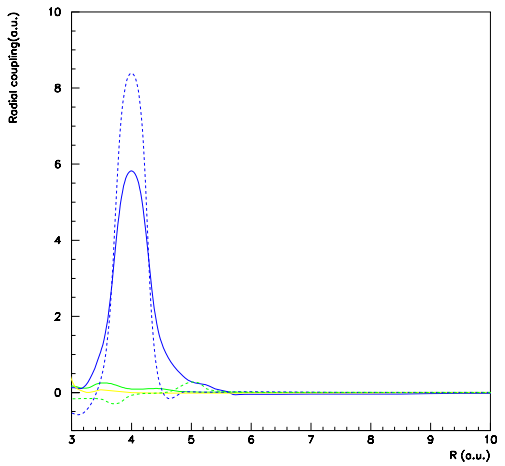

FIG. 9. (Color online) Variation of the g_{23} radial coupling matrix element between $^1\Pi$ levels for different orientations of the C^{2+} projectile toward the CO molecule at equilibrium. Same labels as in Fig. 2. —— α=180° (green); —— α=135° (blue); —— α=90° (yellow); - - - - α=45° (blue); - - - - α=0° (green).

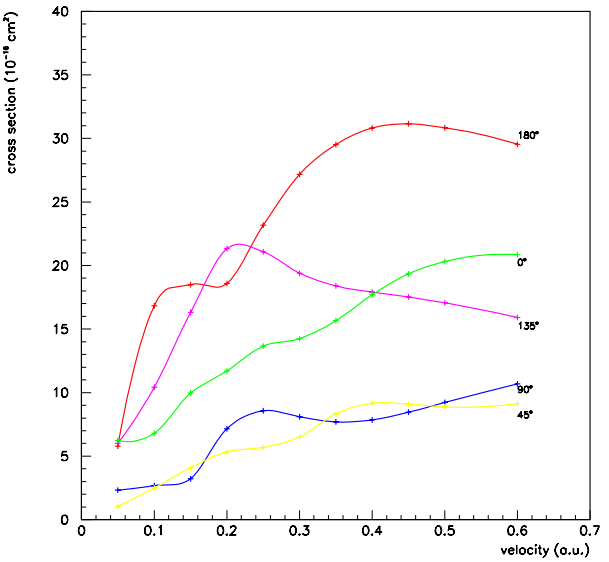

FIG. 10. (Color online) Charge transfer cross sections for different orientations of the C^{2+} projectile toward the CO molecule at equilibrium.

g_{34} radial coupling matrix elements between the $^1\Sigma^+\{C^+(1s^22s^22p)^2P+CO^+(B\ ^2\Sigma^+)\}$ level and the entry channel are very close one to another for the different r_{CO} distances, respectively, r_{CO}=[2.3, 2.140 535 31 (equilibrium), 2.0] a.u., in the linear approach of C^{2+} toward the oxygen atom (α=180°). They present only a very small increase in amplitude with increasing r_{CO} distance, but at the same internuclear distance R=6.5 a.u.. We do not observe the important increase of radial couplings pointed out for the C^{2+}+OH collision system, in the same linear geometry [9]. Consequently, the variation of the cross sections for the different r_{CO} values presented in Fig. 14 is smoother in relative values. In particular, the cross sections are very close one to another

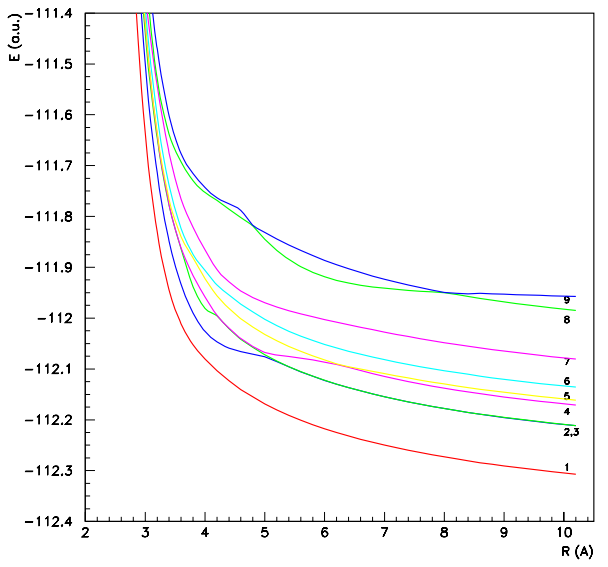

FIG. 11. (Color online) Potential energy curves for the $^2\Pi$ states of the C^{2+}-OH molecular system at equilibrium, α=0°. Same labels as in Fig. 5.

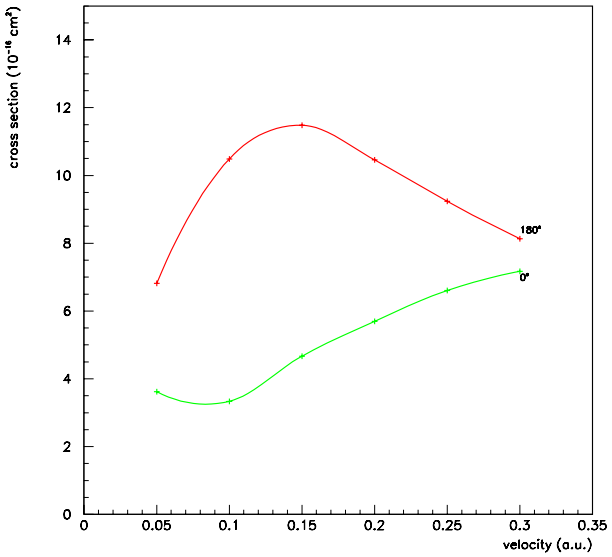

FIG. 12. (Color online) Charge transfer cross sections for different orientations of the C^{2+} projectile toward the OH radical at equilibrium.

between the equilibrium distance and the r_{CO}=2.0 a.u. distance. They show a more significant variation between the equilibrium distance and r_{CO}=2.3 a.u. in correspondence with the sharper radial coupling peak observed at this distance.

The previous study on the collision of the C^{2+} ion on the OH radical in the linear α=180° orientation has been completed to see the influence of the variation of the r_{OH} distance for the linear approach toward hydrogen (α=0°). The results presented in Fig. 15 show a regular increase of the cross sections with increase of the r_{OH} distance. The effect is relatively important in relative value, somewhat higher than in the previous α=180° geometry [9]. A specific mechanism observed for α=180° at very constrained r_{OH} distances is not clearly exhibited in that approach; the vibration of OH being apparently more regular.

TABLE II. Charge transfer cross sections averaged over different orientations for the C^{2+}+CO and C^{2+}+OH collision systems (in 10^{-16} cm^2).

Velocity (a.u.)	E_{lab} (keV)	C^{2+}+CO	C^{2+}+OH
0.05	0.75	4.28	5.22
0.1	3	7.85	6.91
0.15	6.75	10.42	8.07
0.2	12	12.82	8.08
0.25	18.75	14.43	7.92
0.3	27	15.08	7.65
0.35	36.75	15.92	
0.4	48	16.69	
0.45	60.75	17.12	
0.5	75	17.26	
0.6	108	17.22	

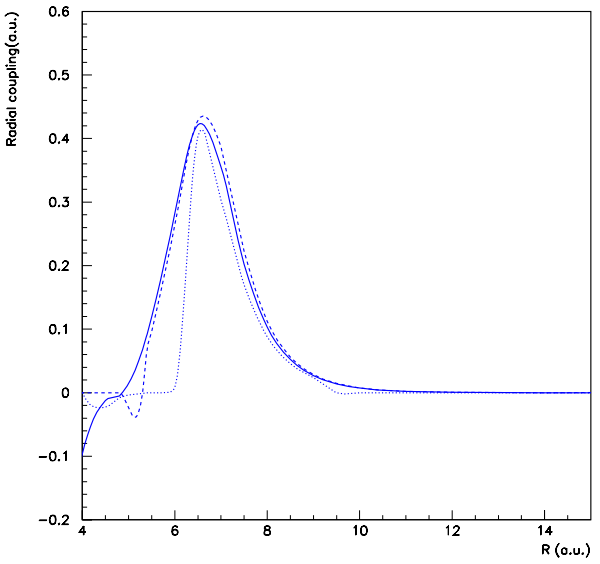

FIG. 13. (Color online) Variation of the g_{34} radial coupling matrix element between $^1\Sigma^+$ levels for different values of the r_{CO} distance for the linear collision C^{2+}+CO, α=180°. Same labels as in Fig. 2. r_{CO}=2.3 a.u., dotted line; r_{CO}=2.140 535 31 a.u. (equilibrium distance), full line; r_{CO}=2.0 a.u., broken line.

IV. CONCLUDING REMARKS

We present a detailed work on the charge-transfer processes induced by collision of the C^{2+} projectile ions on the CO molecule and OH radical. This comparative study exhibits several interesting points which appear to be relatively general in these ion-molecule collisions. First of all, the rotational coupling effect appears to be negligible in both cases for velocities lower than v_{coll}=0.3 a.u., corresponding to a collision energy E_{lab}=27 keV, and rotational couplings could thus be neglected with a correct accuracy for reactions

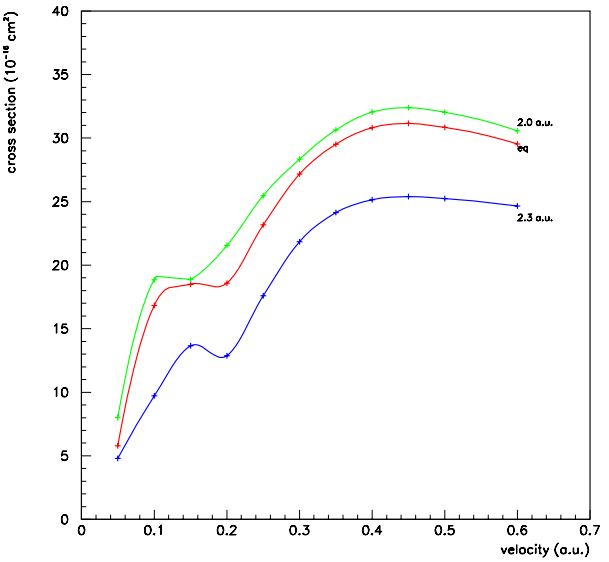

FIG. 14. (Color online) Charge transfer cross sections for different values of the r_{CO} distance for the linear collision C^{2+}+CO, α=180°.

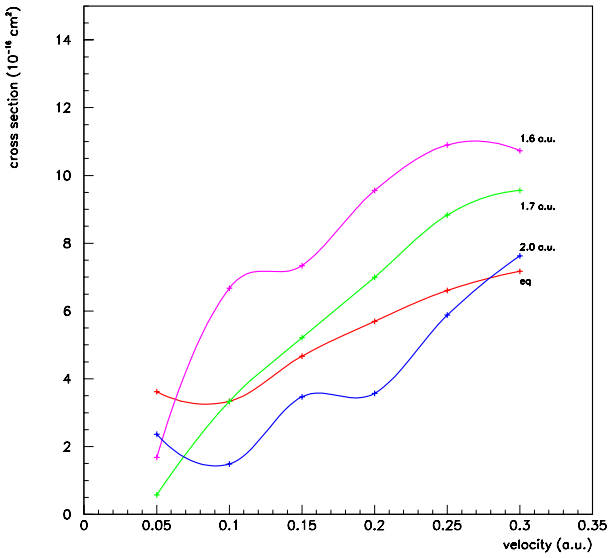

FIG. 15. (Color online) Charge transfer cross sections for different values of the r_{OH} distance for the linear collision C^{2+}+OH, α=0°.

under about E_{lab}=30 keV, in particular in the case of complex molecular systems as C^{2+}+OH. The collision process is highly anisotropic and the charge transfer is clearly favored in the linear approach with reaction of the C^{2+} ion toward the oxygen atom. The vibration effect appears relatively smooth in both cases around the equilibrium distance of the molecular target. Such conclusions could be applied in further studies in order to provide a rapid overview of an ion-molecule charge-transfer process.

ACKNOWLEDGMENTS

The computing facilities of IDRIS (Project No. 81566) and John-von-Neumann Institute, Research Centre Juelich are gratefully acknowledged as well as the support of the COST action P9 "Radiation Damage in Biomolecular Systems" and the Hungarian National Science Foundation OTKA (Project No. TO46905). The authors thank for the French-Hungarian and Spanish-Hungarian bilateral Projects No. 14042UF/F-19/2006 and No. ESP-40/2006.

[1] B. D. Michael and P. D. O'Neill, Science **287**, 1603 (2000).
[2] F. Alvarado, S. Bari, R. Hoekstra, and T. Schlatölter, J. Chem. Phys. **127**, 034301 (2007).
[3] J. de Vries, R. Hoekstra, R. Morgenstern, and T. Schlathölter, Phys. Rev. Lett. **91**, 053401 (2003).
[4] R. Cabrera-Trujillo, E. Deumens, Y. Ohrn, O. Quinet, J. R. Sabin, and N. Stolterfoht, Phys. Rev. A **75**, 052702 (2007).
[5] M.-C. Bacchus-Montabonel, M. Łabuda, Y. S. Tergiman, and J. E. Sienkiewicz, Phys. Rev. A **72**, 052706 (2005).
[6] M.-C. Bacchus-Montabonel and Y. S. Tergiman, Phys. Rev. A **74**, 054702 (2006).
[7] M.-C. Bacchus-Montabonel, Y. S. Tergiman, and D. Talbi, Phys. Rev. A **79**, 012710 (2009).
[8] M. Spotheim-Maurizot, M. Bergusova, and M. Charlier, Actual. Chim. **11-12**, 97 (2003).
[9] E. Bene, Á. Vibók, G. J. Halász, and M. C. Bacchus-Montabonel, Chem. Phys. Lett. **455**, 159 (2008).
[10] H. J. Werner and P. Knowles, MOLPRO (version 2006.1) package of *ab initio* programs.
[11] D. E. Woon and T. H. Dunning, Jr., J. Chem. Phys. **98**, 1358 (1993).
[12] K. P. Huber and G. Herzberg, *Molecular Spectra and Molecular Structure IV. Constants of Diatomic Molecules* (Van Nostrand Reinhold, New York, 1979).
[13] N. Honjou and E. Miyoshi, Chem. Phys. **212**, 363 (1996).
[14] A. Rosén, D. E. Ellis, H. Adachi, and F. W. Averill, J. Chem. Phys. **65**, 3629 (1976).
[15] N. I. S. T. Atomic Spectra Database Levels Data, http://physics.nist.gov/cgi-bin/AtData/main_asd
[16] R. J. Allan, C. Courbin, P. Salas, and P. Wahnon, J. Phys. B **23**, L461 (1990).
[17] B. H. Bransden and M. R. C. McDowell, *Charge Exchange and the Theory of Ion-Atom Collisions* (Clarendon Press, Oxford, 1992), pp. 63–64.
[18] S. Kravis, H. Saitoh, K. Okuno, K. Soejima, M. Kimura, I. Shimamura, Y. Awaya, Y. Kaneko, M. Oura, and N. Shimakura, Phys. Rev. A **52**, 1206 (1995).
[19] L. F. Errea, J. D. Gorfinkiel, C. Harel, H. Jouin, A. Macías, L. Méndez, B. Pons, and A. Riera, Phys. Scr., T **62**, 33 (1996).
[20] P. C. Stancil, B. Zygelman, and K. Kirby, in *Photonic, Electronic, and Atomic Collisions*, edited by F. Aumayr and H. P. Winter (World Scientific, Singapore, 1998), p. 537.
[21] D. R. Bates and R. McCarroll, Proc. R. Soc. London, Ser. A **245**, 175 (1958).
[22] T. G. Winter and G. J. Hatton, Phys. Rev. A **21**, 793 (1980).
[23] L. F. Errea, L. Mendez, and A. Riera, J. Phys. B **15**, 101 (1982).
[24] P. Honvault, M. C. Bacchus-Montabonel, and R. McCarroll, J. Phys. B **27**, 3115 (1994).
[25] H. Lavendy and J. M. Robbe, Chem. Phys. Lett. **205**, 456 (1993).
[26] N. Honjou and D. R. Yarkony, J. Phys. Chem. **89**, 44 (1985).